UDC 57:51-76; 57.02.001.57; 517.958:57

BROWNIAN MOTION SIMULATION OF VESICLE ACTIN TAIL FORMATION

A. I. Oleinick

KNURE, Kharkov, Ukraine, oleinick@kture.kharkov.ua

The mathematical model of actin tail formation at the surface of a spherical vesicle is proposed in this article. The simulation of the protein diffusion process, which is complicated by the formation of a protein cluster at the vesicle surface leading to the development of an actin tail, was performed using the Brownian motion approach. Two relevant mechanisms of tail growth are considered and discussed.

VESICLE, BROWNIAN MOTION, PROTEIN DIFFUSION, CLUSTERISATION, ACTIN TAIL

Introduction

Movement of some vesicles inside the cell occurs because of the catalysed formation of an actin tail which forces the vesicle to move in a certain direction. For example, the investigations of the Xenopus eggs show that within several minutes from their activation by PMA (Phorbol Myristate Acetate) actin tails appeared at some vesicles (endosome or lysosome) in these cells thus propelling the vesicles in the cytoplasm of the cell [1,2]. This process is related solely to the vesicles since it could be reproduced *in vitro*, i.e. out of the cell environment. In previous works [1,2] it was assumed that the origin of this process is the gathering (by diffusion) and growth of the protein (N-WASP/Cdc42 complexes) population in specific regions of the vesicle surface. As a result of this sequence actin tails begin to grow from these regions. However the relationship between the rate of tail growth and rate of protein accumulation at the vesicle surface is still unknown since experimentally one can observe only the rate of actin tail growth.

The aim of this work is to delineate the relation between the rate of tail growth and the rate of protein agglomeration (or its amount) in order to quantify these processes.

1. Mathematical model

Let us consider a vesicle or any other appropriate object enclosed in a membrane (e. g., endosome or lysosome). In the following we will assume it to be spherical with radius ФОРМУЛА. This does not affect the generality of the results presented below unless some shape features significantly alter the probability of the protein displacement or reaction ability. We also assume that N_0 proteins are present in the vesicle membrane, which initially are uniformly and randomly distributed over the membrane spherical surface.

The cytoskeleton structures create nanometric compartments at the vesicle surface [3]. The proteins can move freely and randomly within these compartments, but the walls, imposed by the cytoskeleton, restrict protein movement out of these compartments. However a protein molecule can «jump» over these barriers by accumulating some threshold energy $\Delta E^{\#}$. Therefore the displacement of a protein is equivalent to its «jump» diffusion between nanometric compartments, because the mean protein displacement within the compartment is equal to zero. If the temperature (T) is fixed, the frequency of these jumps is controlled by the Gaussian probability $\exp(-\Delta E^{\#}/k_B T)$ and represents the local diffusion coefficient (D).

Hence in the following we will consider the Brownian motion of proteins over a spherical surface. The Brownian motion of free proteins continues till they become activated by specific cell pathways. The latter provoke a cascade of reactions leading to the formation of a cluster of the N-WASP/Cdc42 protein complexes on the vesicle surface coupled with the activation of Arp2/3 complex and beginning of actin nucleation [1,2]. The main features of the utilised algorithm of Brownian motion are the following. During the free stage of their movement the proteins are considered as rigid cylinders with radius r_{pr} on the vesicle surface and they are not allowed to intersect. At the aggregation phase (i.e. during the formation of a cluster) each protein which approaches the cluster closer than to within r_{react} (the distance between cylindrical surfaces) joins the cluster, i.e. the aggregation rate constant k_{aggr} is assumed to be sufficiently high. When the aggregation phase begins the first two proteins which appear at the required distance and are able to react form the cluster.

It should be noted that such diffusion limited aggregation process will lead to the formation of branched fractal clusters [4]. However in this work we will assume that the cluster always represents a spherical segment with the area equal to the area of the aggregated proteins. The latter assumption has a significant biological basis since it is known for this kind of structures that they possess the ability of regrouping to avoid the forms with long branches [5]. Moreover this statement is also confirmed by electron microscopy images [1].

The elementary step of each protein on a sphere was implemented in a computer program on the basis of the algorithm described in [6] which consists in the following. Let x be a vector which represents the position of the protein on a sphere and contains its Cartesian coordinates. First, a random 3D vector ζ is generated. Each coordinate of this vector is generated using the Gaussian normal distribution with zero mean and a standard deviation $\sigma = 1$ (in fact the outcome of this process does not depend on the precise value

of σ). Then the vector ζ undergoes the orthonormalisation procedure with respect to vector x (i. e. made orthogonal to vector x and is normalized to a unit length):

$$\bar{\zeta}_i = \zeta_i - (\zeta \circ x)\, x_i , \tag{1a}$$

$$\zeta_{ort} = \frac{\bar{\zeta}}{|\bar{\zeta}|} , \tag{1b}$$

where $(\circ)$ denotes the inner product of two vectors. Vector ζ_{ort} defines the direction of the protein displacement. The new position of the protein (x') is calculated according to the following expression:

$$x' = x + \delta\, \zeta_{ort} , \tag{2}$$

where δ is a normally distributed random quantity with zero mean and a standard deviation $\sigma = 2\sqrt{D\Delta t}$.

When the new coordinates of the protein have been evaluated they are tested for acceptability (i. e. the cylinders representing the proteins should not intersect). If the step was not accepted the protein remains at the location where it arrived during the previous time step. After that the protein is checked for its ability to aggregate with the cluster. Since the cluster is represented by a spherical segment and the number of clustered proteins and their area are known, one can easily evaluate the angle corresponding to the cluster edge (θ_{cl}) assuming that its centre is located at the north pole of the sphere. Indeed, the area of the cluster (S^{aggr}) is given by

$$S^{aggr} = 2\pi r_{ves}^2 (1 - \cos\theta_{cl}) , \tag{3a}$$

$$\theta_{cl} = \arccos\left[1 - \frac{S^{aggr}}{2\pi r_{ves}^2} \right] . \tag{3b}$$

The use of dimensionless coordinates (i. e. when all the coordinates and characteristic dimensions are scaled with respect to the vesicle radius, which results into consideration of a unit sphere) coupled with the latter relation allows one to check only the z-coordinate of the particle when deciding whether the particle can join the cluster or not. This fact allows a significant acceleration of the simulation process.

Iterative repeating of the described procedure for all proteins until the required duration of the experiment (t_{exp}) is achieved or all the proteins are aggregated, yields the number of aggregated proteins as a function of time, i. e. the dependence $N(t_k)$, where t_k are the acquisition times. However the available experimental data are given in the form of actin tail length vs. time [2]. Hence it is necessary to establish the correspondence between these two transients. The correspondence law contains fundamental information about how the rate of «comet tail» growth and size of the cluster (or its variation) are linked. Therefore formulating an appropriate correspondence law between the mentioned above transients and its verification will allow one to disclose the exact mechanism of tail formation.

The vesicle comet tail growth transients demonstrate a wide range of behaviours depending on the exact conditions of the experiment. Up to now there are two main hypothetic mechanisms which are considered by the experts in the field [2]. These hypotheses are the following.

1) The growth rate is proportional to the number of clustered proteins, i. e.

$$\frac{dL}{dt} = k_1 N , \tag{4a}$$

where k_1 is the rate constant (in cm/s) whose value corresponds to the growth rate stimulated by one protein. Hence the tail length can be computed on the basis of the $N(t)$ curve as follows:

$$L(t) = k_1 \int_0^t N(\tau)\, d\tau , \tag{4b}$$

where τ is a dummy variable.

2) The growth rate is proportional to the number of proteins which join the cluster through its perimeter per unit of time:

$$\frac{dL}{dt} = k_2 \frac{dN}{dt} , \tag{5a}$$

where k_2 is the rate constant (in cm) whose value corresponds to the tail length supported by one protein. The integration of the latter equation shows that the tail length in this case is proportional to the number of clustered proteins (i. e. $L \sim N$):

$$L(t) = k_2 N(t) . \tag{5b}$$

2. Results and discussion

We refer to the experimental data given in [2]. However before the discussion of experimental data and simulation results let us consider some features of the system at hand. The paper [2] contains plots of the actin tail growth dynamics for glass beads covered with the lipid bilayer containing all the components required for the tail growth. The estimated number of N-WASP proteins is around 50000 of molecules per square micrometer with a maximum distance of 5 nm between the molecules. Using these data we can evaluate the average area available for each protein:

$$\frac{1\,\mu m^2}{5\times 10^4} = \frac{10^6\,nm^2}{5\times 10^4} = 20\,nm^2 . \tag{6}$$

Assuming square packing of proteins in the cluster (for other packings an additional factor commensurable to unity will appear, which, however, does not change the present analysis [7]) and ignoring for the time being the sphericity of the system, we deduce from the latter equation that the size of the packed array cell, and hence the distance between the protein centres, is equal to $a = \sqrt{20\,nm^2} \approx 4.5$ nm . This value shows that the protein radius (r_{pr}) is at most a few nanometers.

The radius of the glass beads employed in the experiments was approximately 1 μm [2]. This implies that the overall number of proteins located at the bead surface, N_0, is:

$$N_0 = 4\pi\ \mu m^2 \times 5\times 10^4 \frac{\text{molecules}}{\mu m^2} = \\ = 6.3\times 10^5\ \text{molecules}. \quad (7)$$

Using such a large number of particles in simulations is extremely time consuming. In order to overcome this difficulty we rely on the approach utilizing quasi-particles, i.e. whenever the number of particles (N_{part}) used in the simulations is less than the number of proteins in the real system (N_0), each particle is considered as a collection of $w = N_0 / N_{part}$ proteins (we also will say that a particle has weight w). The radius of such a weighted particle is evaluated as $\sqrt{w}\, r_{pr}$, i. e. it occupies the same area on the vesicle surface as a collection of proteins which it represents. Simulations results given below were obtained for $w = 600$, since this value was sufficient to achieve convergence in w as was checked by numerical experiments.

It should be noted also that the use of weighted particles also requires scaling of other relevant parameters, in our case of r_{react}. However the clusterisation algorithm described above allows neglecting this scaling since r_{react} and r_{pr} are decoupled because they are not encountered simultaneously in the aggregation condition and only r_{react} and the coordinates of the quasi-particle matter here. Another important parameter is the sampling time (dt). However the used algorithm does not impose a severe condition on its value as was established by inspecting the time convergence. Therefore the sampling time was chosen in order to produce an average particle displacement $\Delta l = 2\sqrt{D\Delta t}$ to be a few (2-3) times larger than r_{react}, but not exceeding the average distance between the particles (l) which is given by

$$l = \sqrt{\frac{4\pi r_{ves}^2}{N_{part}}}\ . \quad (8)$$

For the results given below the following parameters were used: $t_{exp} = 3600$ s, $r_{ves} = 1$ μm, $D = 5\times 10^{-13}$ cm^2/s, $r_{pr} = 2$ nm, $r_{react} = 4$ nm, $N_0 = 6\times 10^5$, $N_{part} = 10^3$. Note that the value of the diffusion coefficient was taken to be smaller than the lateral diffusivity of lipids in the membrane which is generally of the order of $10^{-8} - 10^{-10}$ cm^2/s.

Figures 1 and 2 illustrate the actin tail growth dynamics computed on the basis of $N(t)$ curves according to equations (4) and (5), respectively. The $N(t)$ curves were obtained by averaging ten individual runs of Brownian motion simulations with the same set of parameters. It should be noted that the amplitude of these transients is controlled by the rate constants defined in Eqs. (4)–(5). For the results given in Figures 1 and 2 their values ($k_1 = 3\times 10^{-8}$ μm/s, $k_2 = 6.14\times 10^{-5}$ μm) were adjusted in order to produce the tail length of several tens of microns per hour since this is the inherent growth rate for the system at hand [2]. However despite the same amplitude at the end of the experiment both dependences behave in two qualitatively different ways.

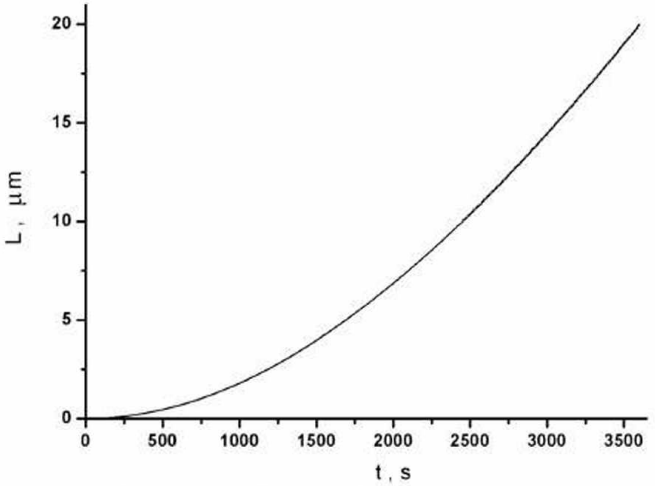

Fig. 1. Tail growth transient obtained via Eq. (3), i. e. growth rate is proportional to the number of aggregated proteins, $k_1 = 3\times 10^{-8}$ μm/s

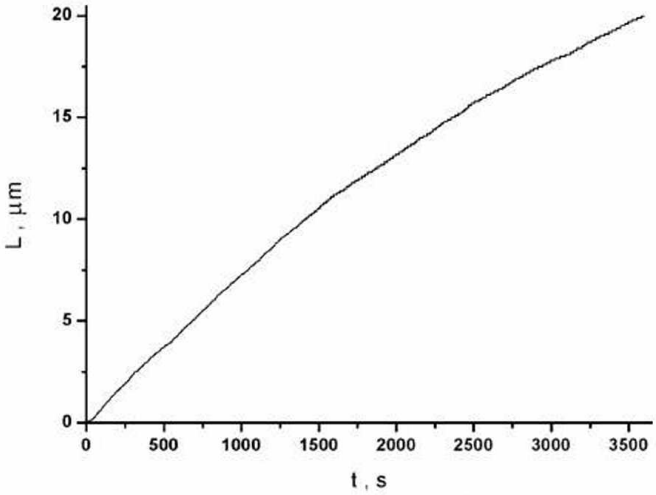

Fig. 2. Tail growth transient obtained via Eq. (4), i. e. tail length is proportional to the number of proteins in the cluster, $k_2 = 6.14\times 10^{-5}$ μm

Indeed, since each aggregated protein steadily increases the tail length, the first mechanism (Figure 1) results in an ever faster growing curve with an asymptote $L \sim k_1 N_0 t$. On the other hand, the curve obtained via the second mechanism (Figure 2) clearly shows the exhaustion of the protein population with time leading to a stationary value of the actin tail length at large times. The latter behaviour is reminiscent to the one observed experimentally (see Figure 5D in [2]). At the same time the behaviour obtained with the first mechanism clearly does not have place at least under the conditions described in [2].

For more precise data fitting more accurate experimental data are required since each reported curve in [2] was obtained from 10-15 experimental curves and, as a consequence of such poor statistics, has sufficiently large error bars. However these data are sufficient for excluding one of the possible mechanisms on qualitative grounds.

Conclusions

The mathematical model introduced in this work describes complex processes involved in the actin tail formation at the vesicle living membrane. The proposed approach to the simulation of the considered problem can be easily modified to account for other mechanisms or interactions if anything of the like is discovered experimentally. Hence it can serve as a basis for the investigation of more general and complex biological phenomena.

Owing to this mathematical model two existing hypotheses of actin tail growth kinetics could be tested: i) the growth rate is proportional to the number of clustered proteins; ii) the growth rate is proportional to the number of proteins which join the cluster per unit of time. The results of this test lead to the conclusion that the first hypothetical mechanism cannot occur in practice (at least it is not observed in experimental data under the conditions given in [2]).

References: **1.** *J. Taunton, B.A. Rowning, M.L. Coughlin, M. Wu, R.T. Moon, T.J. Mitchison, C.A. Larabell.* Actin-dependent propulsion of endosomes and lysosomes by recruitment of N-WASP // Journal of Cell Biology.– 2000.– 148.– pp. 519-530. **2.** *C. Co, D.T. Wong, S. Gierke, V. Chang, J. Taunton.* Mechanism of actin network attachment to moving membranes: barbed end capture by N-WASP WH2 domains // Cell.– 2007.– 128.– pp. 901–913. **3.** *A. Kusumi, C. Nakada, K. Ritchie, K. Murase, K. Suzuki, H. Murakoshi, R. S. Kasai, J. Kondo, T. Fujiwara.* Paradigm shift of the plasma membrane concept from the two-dimensional continuum fluid to the partitioned fluid: high-speed single-molecule tracking of membrane molecules // Annu. Rev. Biophys. Biomol. Struct. 34, 2005, pp. 351-378. **4.** *P. Pelce.* New visions on form and growth.– Oxford University Press, 2004.– 388 p. **5.** *A. Lehninger.* Principles of Biochemistry.– W. H. Freeman & Co, 2004.–1110 p. **6.** *W. Krauth.* Statistical Mechanics: Algorithms and Computations.– Oxford University Press, 2007.– 320 p. **7.** *C. Amatore.* Is there an Intrinsic Limit to the Size of 2D Supracrystals Built from Weakly Interacting Nanoparticles? // Chem. Eur. J.– 2008.– 14(28).– pp. 8615-8623.

Поступила в редколлегию 27.02.2009

УДК 57:51-76; 57.02.001.57; 517.958:57

Моделирование роста актинового волокна у везикул при помощи броуновского движения / А.И. Олейник // Бионика интеллекта: науч.-техн. журнал.– 2009.– № 1 (70).– С. 82–85.

В статье предложена математическая модель роста актинового волокна на поверхности везикулы и дано количественное описание данного процесса с использованием броуновского движения. Рассмотрены два гипотетических механизма образования актинового волокна, известные из литературы. Сравнение результатов моделирования, соответствующих этим механизмам с экспериментальными данными, позволили сделать заключение, что один из механизмов не приводит к поведению, наблюдаемому в эксперименте.

Ил.: 2. Библиогр.: 7 назв.

УДК 57:51-76; 57.02.001.57; 517.958:57

Моделювання росту актинового волокна у везикул за допомогою броунівського руху / О.І. Олійник // Біоніка інтелекту: наук.-техн. журнал. –2009. –№ 1(70). –С. 82–85.

У статті запропоновано математичну модель росту актинового волокна на поверхні везикули та наведено кількісний опис цього процесу з використанням броунівського руху. Розглянуто два гіпотетичних механізми створення актинового волокна, що відомі з літератури. Порівняння результатів моделювання, що відповідають цим механізмам, з експериментальними даними дозволило зробити висновок, що один з механізмів не призводе до поведінки, яка спостерігається в експерименті.

Іл.: 2. Бібліогр.: 7 найм.